ADVANCED MATERIALS TECHNOLOGIES
www.advmattechnol.de

New Approach for Enhancing Sensitivity in Liquid-Gated Nanowire FET Biosensors Under Optical Excitation

*Mykhailo Petrychuk, Denys Pustovyi, Nazarii Boichuk, Yongqiang Zhang, Hanlin Long, and Svetlana Vitusevich**

The results obtained for liquid-gated (LG) nanowire (NW) field-effect transistor (FET) sensors analyzed in divalent ion ($MgCl_2$) solutions, which play a crucial role in the human body, are reported. Liquid-gated NW FET sensors fabricated in-house are investigated using *I–V* characteristics and noise spectroscopy in a wide range of voltages and different intensities of optical infrared irradiation. A new effect is revealed under the influence of external optical excitation. The effect allows for the control of characteristic times of single-trap phenomena: capture time to a single trap, emission time from the trap, and its ratio represented by the dimensionless ratio parameter (R-factor). These parameters enabled an improvement in sensor sensitivity. The findings open prospects for controlling charge states in LG NW FET structures to optimize new parameters for achieving ultrahigh sensitivity in biosensors.

1. Introduction

Liquid-gated (LG) nanowire (NW) field-effect transistors (FETs) are key biochemical sensors[1–3] due to their rapid detection of biomarkers and ultrahigh sensitivity down to the 20 *fM* level. This could allow diseases to be monitored at a predictable stage and the balance state to be restored even with small deviations from the normal state. Currently, there is an active search underway to implement and utilize new effects and parameters[4–8] in order to improve the capabilities of LG NW FET sensor calibration, further increase the sensitivity, and process the biological signals more reliably. Nanoscale sensors are promising devices in this respect. They might not only allow for studies and usage of new transport regimes but also a demonstration of several advantages, including a more sensitive, high-speed detection of biochemical signals[9–14]

M. Petrychuk, D. Pustovyi, N. Boichuk, Y. Zhang, H. Long, S. Vitusevich
Institute of Biological Information Processing (IBI-3)
Forschungszentrum Jülich
52425 Jülich, Germany
E-mail: s.vitusevich@fz-juelich.de

The ORCID identification number(s) for the author(s) of this article can be found under https://doi.org/10.1002/admt.202301303

DOI: 10.1002/admt.202301303

We have recently shown that singe-trap phenomena (STP) and noise properties of LG NW FETs might offer new time parameters[15–21] for biosensing applications. Using the capture time to a single trap near a semiconductor channel and the characteristic emission time enables sensitivity to be improved. It was demonstrated that the sensitivity of NW FETs in solutions with monovalent ion systems (e.g., KCl and NaCl) can be enhanced by 300% or more through the utilization of STP and new detection parameters, which are referred to as characteristic time parameters.[16] In addition, the two-level signal, which can be considered as a digital switching signal, makes it possible to extract the useful signal from the noise.[22] Studies on the possibility of fine-tuning characteristic times and the optimal choice of time range currently represent an unexplored area of research.

In this paper, we present the results of studies on the influence of external optical radiation on the transport and noise properties of LG NW FETs operating in magnesium chloride ($MgCl_2$)solutions. It should be emphasized that $MgCl_2$ solutions play a crucial role in many enzymatic reactions, such as DNA folding. A change in its concentration in human body solutions (blood, serum, saliva) might reflect a gastrointestinal disorder: the disease or syndrome.[23,24] NW FET structures are designed for use as sensitive elements of biosensors. Several samples with liquid gates (LGs) were investigated. In the liquid medium ($MgCl_2$ solutions), the $Ag/AgCl_2$ reference electrode was used to apply voltage to the liquid gate of FET structures with a volume for a liquid. The impact of light excitation on the properties of a unique nanowire NW FET utilizing single-trap phenomena was studied. Under the influence of optical radiation, the population of carriers on energy levels is redistributed, which allows their energy characteristics to be controlled and thus establishes optimal sensitive regimes. It should be noted that the influence of light on the trap parameters in liquid-gated FET structures has not been reported in the literature.

2. Results and Discussion

Typical liquid-gated NW FET structures under investigation are schematically shown in **Figure 1**A. It should be noted that in our experiment absorption and scattering of light in the solution are negligibly small. The minimization of these factors was achieved

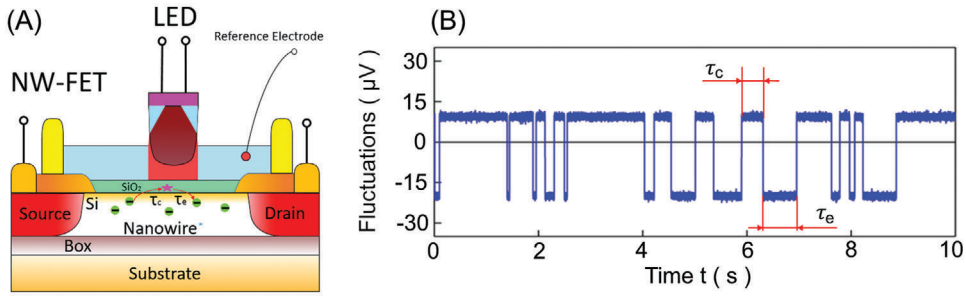

Figure 1. A) Schematic presentation of liquid-gated (LG) FET under external optical excitation. The layer structure includes an 8 nm SiO_2 dielectric layer, a 50 nm thick Si nanowire, a 145 nm buried oxide (BOX) layer, 700 μm heavy-doped silicon substrate. B) Typical time trace of RTS noise for the LG nanowire FET structure, measured at room temperature, IR light of 80 mW cm^{-2}. Capture time τ_c and emission τ_e constants in the channel of the LG NW FET structure with a width of 100 nm and a length of 200 nm (measured in the dark) obtained for a 10^{-6} M $MgCl_2$ solution at $V_{LG} = -0.75$ V.

by immersing the LED in the solution, which allows minimizing the distance to the sensitive surface and eliminates the influence of meniscus geometry as well. Time traces of drain current fluctuations as a function of time are recorded using an experimental setup developed in-house. A periodical change in drain current level is recorded (Figure 1B) as a result of a single trap, usually situated in a dielectric layer at a distance of 0–2 nm from the Si/SiO_2 interface, which randomly captures or emits a hole from the NW conducting channel.

The two-level voltage steps are well resolved due to the modulation of channel current by a value exceeding one charge carrier, which in turn is a result of the change in the electric field around the trap. Here, the capture time t_c and the emission time t_e are random variables. Their average values, τ_c and τ_e, are referred to as capture and emission time constants, respectively:

$$\tau_c = \langle t_c \rangle \ , \ \ \tau_e = \langle t_e \rangle \tag{1}$$

The capture time, t_c, is the time during which the hole is in a free state before it is trapped; the emission time, t_e, is the time during which the hole is bound to the trap before it transitions to the free state. The values τ_c and τ_e in the equilibrium state can be controlled by the concentration of holes in the valence band (p-silicon) according to the law:

$$\tau_c = \frac{1}{C_p p_s} \exp\frac{\Delta E}{kT}, \ \tau_e = \frac{1}{C_p N_v} \exp\frac{E_T}{kT} \tag{2}$$

where C_p is the hole capture coefficient $C_p = \sigma_p \nu_{th}$; σ_p is the hole capture cross-section; ν_{th} is the thermal velocity; p_s is the effective volume concentration of holes at the Si/SiO_2 interface; N_v is the effective density of states at the top of the valence band; E_T is the energy between the trap level and the top of the valence band; and ΔE is the Coulomb blockade energy.

Since the energy required for a transition corresponding to an indirect bandgap is 1.1 eV for silicon, we use light with a shorter wavelength than is required for band–band transitions (1.13 μm) in silicon. An optical radiation with a wavelength of 0.95 μm was selected, which corresponds to a photon energy of 1.3 eV. It should be underlined that the light-emitting diode as a light source was chosen due to its small size, ease of operation, and small price compared to the monochromator as well as due to the relatively higher light power that can be applied to the sensitive element of the sensor. This greatly simplifies the experiment targeted at the design of biosensors. The 950 nm LED light was selected, because our experimental results show that exposure to light with a shorter wavelength leads to degradation of the biosensor. The influence of light excitation on RTS parameters is chosen as a new method of fine-tuning RTS parameters, which may work independently of the applied voltages. In addition, minimizing the voltages applied to the liquid gate sensor is necessary to avoid electrochemical reactions. In this respect, small gate voltages may be used under the influence of light excitation to effectively control the RTS parameters. Thus, to study the influence of optical radiation on RTS fluctuations, a near-infrared (0.95 μm) light-emitting diode (LED) was used. The changes in the time constants of the capture and emission of free charge carriers per single trap were studied by recording current changes through the channel of silicon LG FET structures at different optical intensities.

The E_T, N_v, ΔE, and E_T values in Equation (2) do not change during irradiation. The value of p_s changes slightly since silicon is an indirect bandgap semiconductor and demonstrates a weak photo effect at this length of optical wave. In the equilibrium state, the electron energy is determined by the lattice temperature, but in the nonequilibrium state, during irradiation, the carrier energy increases by the photon energy $h\nu$. The probability of hole transition in such a state depends on the intensity of the light.

Modulation conductivity in metal oxide semiconductor (MOS) FET structures resulting in two-level current fluctuations is explained as a capture/emission process of a free carrier to/from a single trap. For a low-defect density ($\approx 10^{12}$ cm^{-2}) near the interface there is no electrostatic correlation between the traps in the dielectric layer near the Si/SiO_2 as well as between the capture/emission processes of adjacent traps. At the same time, the correlation effect can be registered for a parallel conduction channel, which is electrostatically connected to the main channel, as in the case of high-electron-mobility transistor (HEMT) structures based on GaN/AlGaN.[25] In contrast to traditional, "dry" MOSFET structures, silicon FET structures with a liquid gate have a parallel conduction channel represented by a liquid, i.e., at the interface (Stern layer) between a thin subgate dielectric and the neutral region of the electrolyte. Features of the drift and diffusion of ions in this layer are determined by the specific Coulomb

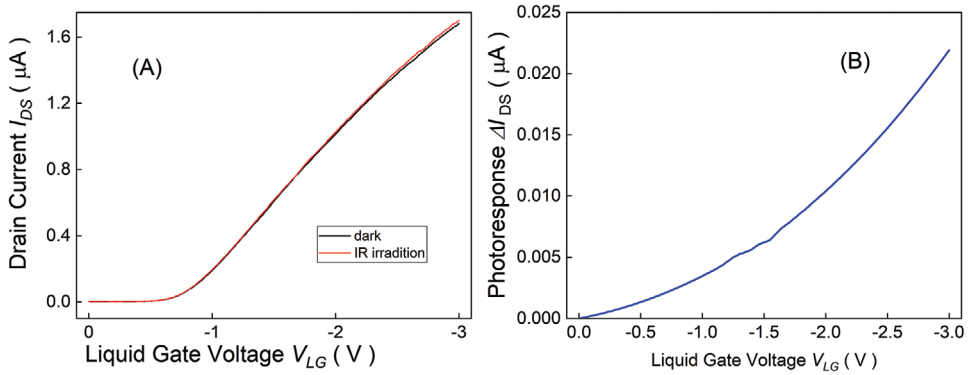

Figure 2. A) Transfer characteristics of a liquid-gated NW FET sample with a width of 100 nm and a length of 200 nm, measured at 80 mW cm^{-2} optical excitation of IR range. B) Photoresponse was obtained as a function of the liquid-gate voltage as a difference current measured at optical excitation by IR light and dark current using the data of (A), measured at $V_{DS} = 0.10V$ in 10^{-6} M $MgCl_2$ solution.

interaction between the ions and the interaction with the charge states at the interface. This effect is accompanied by a significant increase not only in RTS noise but also in level 1/f-noise, i.e., the noise of such structures is extremely sensitive to the situation in the parallel channel. The behavior of both the flicker noise and the RTS noise of FET structures with a liquid gate is thus largely determined by the type of molecules[18] in the electrolyte layer near the interface. They can therefore serve as tools for detecting specific molecules in the liquid.

Based on Equation (2), it is possible to analyze the dependences of the time constants τ_c and τ_e as a function of the gate voltage. At the same time, the influence of optical radiation on fine-tuning to use of digital RTS signal parameters for biosensing applications has not been reported in the literature and should be studied in further detail.

2.1. *I–V* Characteristics of LG NW FETs Under the Influence of IR Radiation

Measurements of FETs with a liquid gate (LG FETs) were performed in 10^{-6} M $MgCl_2$ solution using an Ag/AgCl reference electrode. LG FET structures with a width of 100 nm and a length of 200 nm were studied. Typical *I–V* characteristics of liquid-gated NW FET structures, measured in the dark and under optical excitation, are shown in **Figure** 2A.

Silicon is an indirect bandgap semiconductor material, therefore it demonstrates a very weak photo effect. The conductivity of silicon nanowires thus shows a weak dependence on the level of optical irradiation. The characteristic changes (Figure 2B) do not exceed 1.4%. The effect of photoexcitation can be explained as follows. The photon flow causes a redistribution of charges at the Si/SiO_2/LG interfaces and the system leaves the equilibrium state, which leads to an increase in the charge density at these interfaces. This results in a change in the photoresponses (Figure 2B). We should consider the characteristics of devices that are related to the change of charge states of defect centers in SiO_2. Generation–recombination (G–R) noise is one such characteristic,[26] which is caused by charge fluctuations in the SiO_2 layer. G–R-noise in small devices is determined by charge fluctuations at a single center, which allows changes in liquid-gate potential to be recorded with high sensitivity in a wide voltage range.

As can be seen in Figure 2, the excitation of silicon material with wavelengths corresponding to indirect transitions results in a very weak photoeffect with low efficiency. Recently it was shown that noise characteristics can be used as a signal, not only to analyze the device performance but also to get insight into the dynamic processes in biosensors and assist in obtaining enhanced sensitivity in FET biosensors.[14,16,17,20–22] A considerable change in the noise behavior was revealed when silicon nanowires were irradiated using infrared light as will be shown below.

2.2. Noise Characteristics of LG NW FETs Under the Influence of IR Radiation

Typical results are shown in **Figure 3**. Figure 3A shows the spectra of current fluctuations, measured in LG NW FET at a voltage of $V_{LG} = -0.75$ V at different levels of illumination in the infrared range. One or two Lorentzian-type noise components corresponding to GR noise are present in the spectra:

$$S_I(f) = \frac{S_I(0)}{1 + (2\pi f \tau)^2} \tag{3}$$

where $S_I(0)$ is the current noise spectral density, f is the frequency, and τ is the characteristic time constant corresponding to the Lorentzian-type noise component.

In Figure 3A, noise properties measured for LG NW FETs are shown in the form of noise spectral density multiplied by frequency $fS_I(f)$. This enables a better distinction of the deviation from the $1/f$ law, which describes the flicker noise (denoted by a horizontal line). Two-level fluctuations of drain current are also registered. Lorentzian-shaped noise power spectral density of a single two-level RTS is given by:

$$S_I(f) = \frac{4(\Delta I)^2}{(\tau_c + \tau_e)\left[\left(\frac{1}{\tau_c} + \frac{1}{\tau_e}\right)^2 + (2\pi f)^2\right]} \tag{4}$$

where ΔI is the RTS amplitude, and τ_c and τ_e are the characteristic times for a specific trap level at a given bias condition.

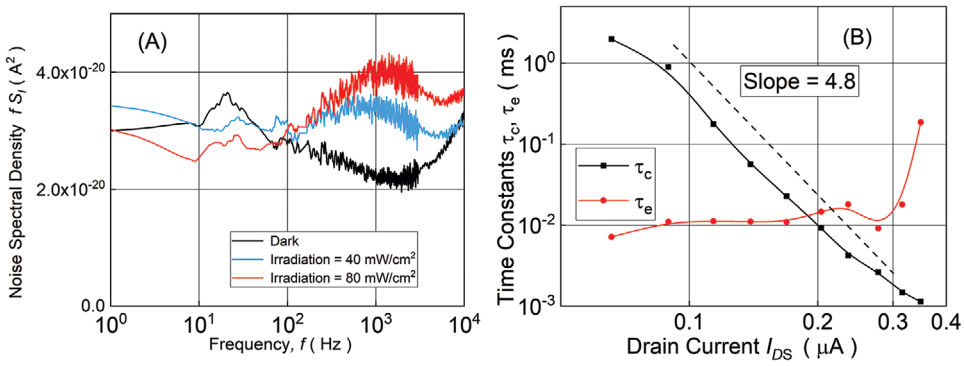

Figure 3. A) The normalized $fS_I(f)$ noise spectra of the LG NW FET with a width of 100 nm and a length of 200 nm at different irradiation levels, normalized to the maximum value, obtained for 10^{-6} M $MgCl_2$ solution at a liquid-gate voltage of $V_{LG} = -0.75$ V. B) Dependences of the capture time τ_c and emission τ_e constants on the current in the channel of the LG FET structure with a width of 100 nm and a length of 200 nm in the absence of irradiation, measured for 10^{-6} M $MgCl_2$ solution.

Since the spectra in Figure 3A reflect charge fluctuations on a single center, it is possible to separate the capture and emission time constants. Each of the spectra in Figure 3 reflects characteristic Lorentzian with maximum at a certain frequency and corresponding time constant τ:

$$\tau = \frac{\tau_c \cdot \tau_e}{\tau_c + \tau_e} \tag{5}$$

Typical dependences of time constants on current in the channel for the case of τ_c ,$\tau_e = f(I_{DS})$ in the absence of irradiation are presented in Figure 3B. The nature of the dependences indicates that in this case, the trap is located in the neutral region of the channel. Time parameters of the trap located in the channel of an LG FET structure were studied in the dark as well as under IR excitation The time constant, τ_c, has a strong dependence on both V_{LG} and illumination intensity (as it will be shown below). In the case where the active center is located in the area of space charge (e.g., in the near-contact area), the value of τ_e may also depend significantly on V_{LG} . In these conditions, the time-constant τ_e can also be an informative parameter.

The slope extracted using Figure 3B for capture time versus drain current (equal to $\gamma = 4.8$) can be used to estimate the amplification coefficient for biochemical signal detection using the STP approach.[16,20,21] For the standard approach, the sensitivity, $S_{(I_D)}$, of a typical LG FET-based sensor is estimated using a change in drain current, ΔI_D, as a function of the change in surface potential, $\Delta\psi_S$, after the attachment of a biomarker[1,2]

$$S_{(I_D)} = \frac{\Delta I_D}{\Delta\psi_S} \tag{6}$$

For the STP approach, the capture rate, which is defined as the reverse capture time, can be used as the sensing parameter and the sensitivity, S^{STP}, can be calculated as follows:[20]

$$S^{STP} = \frac{\Delta\left(1/\tau_c\right)}{\Delta\psi_S} \tag{7}$$

where $\Delta(1/\tau_c)$ is the change in the capture rate after the attachment of a biomarker.

Within the standard Shockley–Reed–Hall (SRH) model[27,28] for a trap in the bulk material, the capture rate, which corresponds to reverse capture time, is as follows:

$$\left(1/\tau_c\right)^{(SRH)} = \sigma_p \, v_{th} p \tag{8}$$

where p is the concentration of free holes in the Si material.

The capture rate is thus proportional to when the concentrations of holes in power equal 1:

$$\left(1/\tau_c\right)^{(SRH)} \sim p^1 \tag{9}$$

For liquid-gated NW FET structures, the total potential $\Psi(x)$ includes: band bending potential $\psi(x)$ and mirror image charge φ(x) potential

$$\Psi\ (x) = \ \psi\ (x) + \varphi\ (x) \tag{10}$$

where x is the position of the mirror image charge related to the Si/SiO_2 interface.

The ψ(x) can be obtained by solving the Poisson equation:

$$\frac{\partial^2 \psi\ (x)}{\partial x^2} = -\frac{q}{\epsilon_s \epsilon_0}\left(p_{p0} e^{-\frac{q\psi}{kT}} - N_A - n_{p0} e^{\frac{q\psi}{kT}}\right) \tag{11}$$

And φ(x) from:

$$\varphi\ (x) = \frac{q}{16\pi\epsilon_0\epsilon_{Si}}\left(\frac{\epsilon_{SiO_2} - \epsilon_{Si}}{\epsilon_{SiO_2} + \epsilon_{Si}}\right)\frac{1}{x} \tag{12}$$

Here, $\epsilon_{SiO2} = 3.9$ $\epsilon_{Si} = 11.7$; ϵ_0 is the vacuum permittivity; and q – is the elementary charge.

The surface potential is a function of the charged ions attached to $MgCl_2$ solutions. The sensitivity for the STP approach can be defined as:

$$S^{STP} = \frac{\Delta\left(1/\tau_c\right)}{\Delta\psi_S} \tag{13}$$

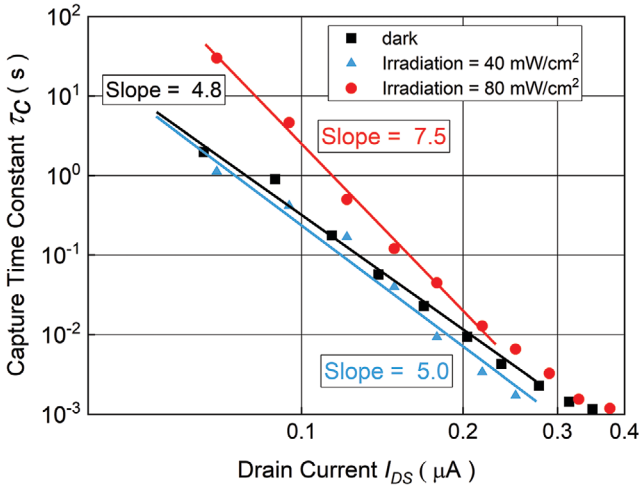

Figure 4. Dependences of the capture time constants, τ_c, on the current in the channel of the LG FET structure with a width of 100 nm and a length of 200 nm, measured in the dark and at different IR light excitations: 40 and 80 mW cm^{-2} at $V_{LG} = -0.75$ V for a 10^{-6} M $MgCl_2$ solution.

where the capture rate is proportional

$$1/\tau_c \sim p_s^{\ \gamma} \tag{14}$$

Here, γ is an exponent of power $\gamma \geq 1$.

An analysis of data from Figure 3B shows that the slope, or value of gamma, γ, in dependence of the capture time constant as a function of the drain current is equal to 4.8. Our results of pH sensitivity and biosensitivity studies using characteristic times of the RTS approach demonstrate a direct relation between this slope and the sensitivity of FET biosensors.[16,20,21] The value of power $\gamma = 4.8$ corresponds to a 480% amplification of the biochemical signal compared to the standard approach, where the change in the charge of the surface of the dielectric of the FET structure affects the value of the current in the channel.[16,21] Under the influence of an IR light intensity of 80 mW cm^{-2} (**Figure 4**), the slope increases to 7.5, corresponding to a 750% amplification.

The ratio of the slope obtained under illumination of 80 mW cm^{-2} to the slope obtained without it is equal to 1.56. Thus, the sensitivity of the liquid-gated sensor increases 1.56 times under light excitation compared to the sensitivity in the dark.

For the characterization of RTS fluctuations due to STP, it is appropriate to introduce the dimensionless R-factor:

$$R = \tau_e/\tau_c \tag{15}$$

The time constants can be precisely obtained from analysis of the corresponding RTS fluctuations using histograms,[29] as shown in **Figure 5**.

When carriers approach the interface, additional energy, referred to as Coulomb blockade energy[30,31] should be considered. The energy is a result of the formation of image charge forces at the interface. The energy ΔE increases the energy required for the free charge to capture the neutral local level in the sub-gate dielectric of the FET structure near the interface. An additional barrier is created (**Figure 6A**)[20] due to the quantization of the levels in the semiconductor and the displacement of the maximum density of free charges in the channel of the structure from the interface.

The quantum mechanical modeling of charge carrier distribution in NW FET biosensors was performed using NextNANO simulation software for semiconductor nanodevices.[32] The results of the numerical calculation of the electron density distribution in the channel are given in Figure 6B, where X_q is the distance between the maximum quantum redistribution of the carriers and the Si/SiO_2 interface position.

As can be seen in Figure 6B, the displacement of the electron density maximum from the interface, which is caused by the quantization of electron energy, leads to the appearance of a region with a reduced concentration of free carriers near the interface. Under the influence of IR light excitation, two processes can be considered. The first–trap state becomes excited and therefore the probability of capturing a carrier changes. The second – the maximum position of quantum redistribution of the carriers changes due to the influence of the Coulomb blockade effect in the region of the trap even for a small photoexcitation and penetration part of the hole wave function into SiO_2 layer changes, respectively.

Despite the small changes in *I–V* characteristics (Figure 2), the noise properties of LG NW FET reflect considerable changes. The frequency characteristics of the GR noise spectrum change strongly (Figure 3A). The frequency position of the Lorentzian maximum obtained in dark (the spectrum shown in black) increases by several orders of magnitude at the light excitation (the spectrum shown in red). Exposure to IR light thus results in non-equilibrium conditions for the formation of current fluctuations. This changes the population of noise centers in the gate dielectric, which are responsible for noise in LG FET structures. The effectiveness of controlling noise characteristics in this way can be explained as follows. The transitions between the trap level in the dielectric and the valence band are straight band ones. Therefore, such transitions are highly efficient. The effect of optical radiation results in the positive shift (Figure 3A) of the noise characteristics of the sample measured under optical excitation of the infrared range (0.95 μm). It increases with the increase in the overdrive voltage. This shows that there is a significant spectral selectivity of the influence of illumination on the charge state of interface centers. The spectra of generation–recombination noise strongly depend on the charge state of an active center, i.e., a center whose energy level is close to the Fermi level in a semiconductor, which leads to active charge fluctuations on this center. The capture and emission times change as a function of the population of this level with a charge carrier. This is reflected in the spectra of these fluctuations and in the form of time sequences of charge fluctuations. If the population of the level changes under the effect of optical irradiation, this is manifested in a change in the shape of the spectrum of fluctuations.

The data shown in **Figure 7A** support the described mechanism. The *R*-factor values, estimated using Equation (15), are plotted as a function of the current in the I_{DS} channel for different levels of infrared light (0.95 μm) irradiations. Under the influence of IR irradiation, the *R*-factor changes by more than an order of magnitude, and the slope of the dependence $R(I_{DS})$ reaches values of 7.8 at an irradiation of 80 mW cm^{-2}. This

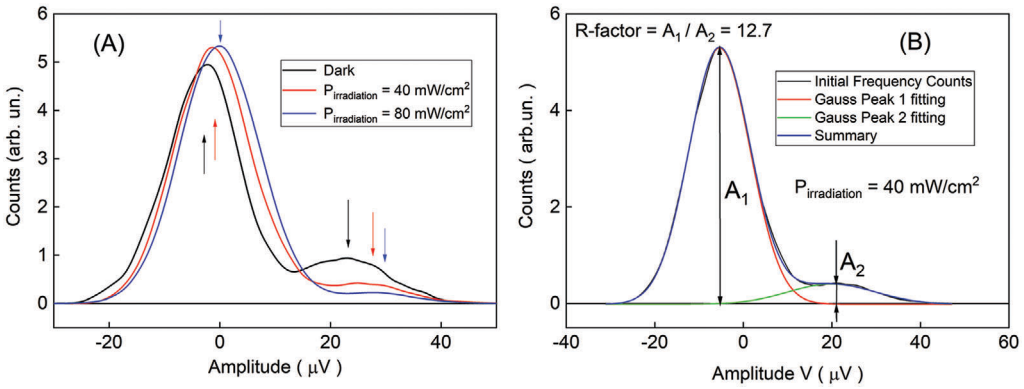

Figure 5. A) Histogram plotted for the analysis of RTS voltage fluctuations of drain current for an LG NW FET biosensor with a width of 100 nm and a length of 200 nm, measured under the influence of IR light (40 and 80 mW cm^{-2}) with a wavelength of 0.95 μm and without it and at $V_{DS} = 0.10V$ in a 10^{-6} M $MgCl_2$ solution. B) Demonstrations of the determination procedure of the R-factor from a histogram A) fitted using two Gaussians for an illumination level of 40 mW cm^{-2}.

reflects the fact that a stronger slope of *R*-factor corresponds to the improved NW FET bio-sensitivity obtained for the new STP approach. The sensitivity of FET biosensors estimated as a ratio of the slopes can thus be amplified by 1.56 times under light excitation compared to the amplification coefficient obtained in the dark. The utilization of trap parameters under conditions of optical irradiation thus makes it possible to significantly increase the sensitivity of the informative parameter to the potential at the surface dielectric in contact with the $MgCl_2$ solution.

When analyzing the effect of light photon irradiation on the dynamics of the generation–recombination process, it should be noted that the charge carrier (electron or hole in our case) fully absorbs the photon energy, as predicted by the theory of the photoeffect. For a first approximation, it can thus be concluded that photon irradiation should lead to a change in the values of the capture time, τ_c, and emission time constants, τ_e, and the probability of photon absorption should therefore increase with increasing irradiation intensity. The experiment confirmed such a phenomenon (Figure 7). The changes in details can be analyzed by calculating the normalized *R*-factor obtained as a ratio of the *R*-factor in the dark, R_0, to the *R*-factor under IR light excitation (Figure 7B). As the current in the channel increases, the sensitivity of the value of the *R*-factor to the irradiation power decreases. However, it should be noted that a change in illumination from 0 to 80 mW cm^{-2} leads to an increase in the normalized *R*-factor by 25 times at $I_{DS} = 0.07$ μA and by 4.3 times at $I_{DS} = 0.2$ μA. The sensitivity to the light excitation of the normalized *R*-factor increases when the voltage V_{LG} approaches the threshold value, at which point $I_{DS} = 0.07$ μA. These parameters are therefore optimal for utilizing the high photosensitivity effect for different applications, including biosensing applications. Results shown in Figure 7 demonstrate that characteristic parameters of RTS responses can be effectively tuned not only by gate voltage but also by optical excitation.

It should be emphasized that a change in the voltage of any gate, like the back gate causes changes in the statistical parameters of RTS fluctuations due to the control of carrier concentration in the channel. At the same time, our results show that the effect of illumination changes these parameters due to the transfer of the FET energy levels to a nonequilibrium state without changing the concentration of mobile carriers in the channel. Therefore, the effect of light excitation has a different nature

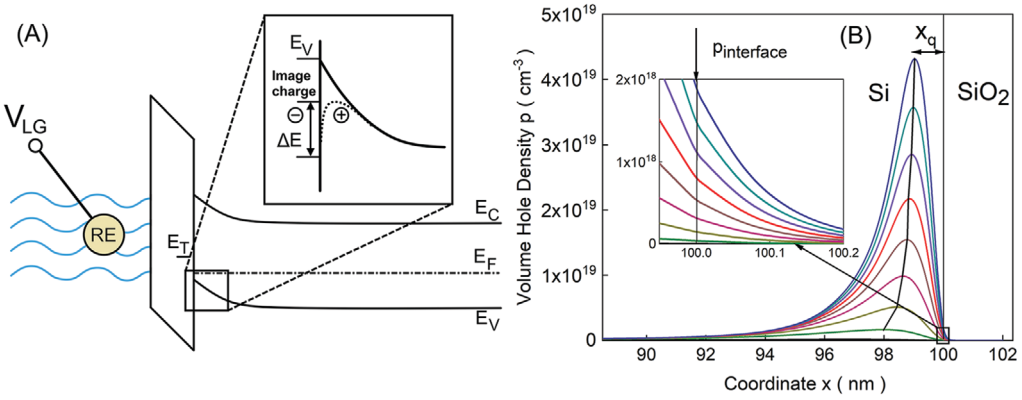

Figure 6. A) The density distribution of free holes in the FET structure near the interface, was calculated using the NextNANO program. The inset shows an enlarged area at the Si/SiO_2 interface in the same coordinates. The concentration of the alloying impurity, $N_D = 10^{15}$ cm^{-3}, n_{int}, is the free-carrier concentration at the Si/SiO_2 interface, which is obtained from $V_{FG} = 0$ V to $V_{FG} = 3.9$ V with a step equal to 0.5 V. B) Schematic representation of the additional barrier due to mirror reflection forces for an LG NW FET structure with a *p*-type channel.

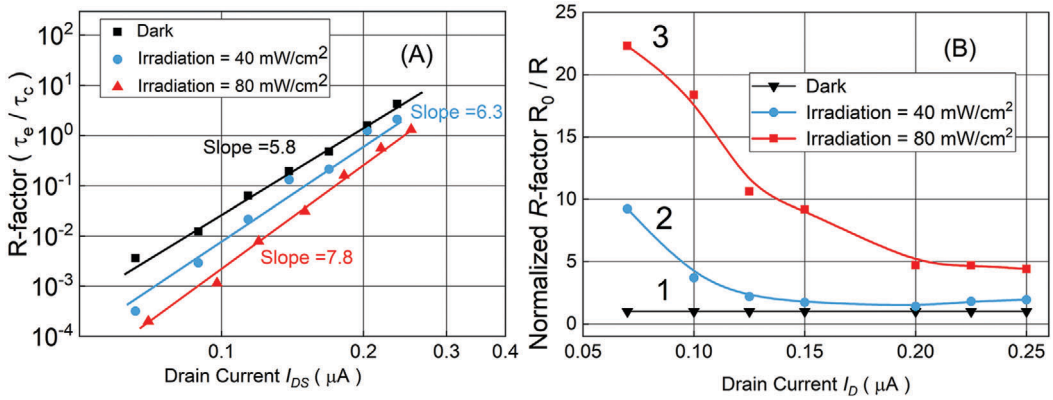

Figure 7. A) Dependencies of the *R*-factor, $R = (\tau_e/\tau_c)$ of an LG NW FET biosensor with a width of 100 nm and a length of 200 nm at different levels of IR LED irradiation ($\lambda = 0.95$ μm), obtained at $V_{DS} = 0.10V$ in a 10^{-6} M $MgCl_2$ solution. The slope at irradiation changes to 7.8 compared to the 5.8 value in the dark, reflecting 1.5 times amplification in biosensitivity. B) Normalized *R*-factor of an LG NW FET biosensor demonstrating sensitivity amplifications under different irradiation powers (mW cm^2): 1–0, 2–40, 3–80.

compared to conventional gating and has different consequences, respectively. Optical excitation in this work is used to study the possible fine-tuning effect on the parameters of RTS fluctuations as sensitive parameters of the biosensor and is aimed at practical application in the designing of new biosensors.

3. Conclusion

The fabricated liquid-gated NW FETs have great potential for advanced biosensors. Noise spectroscopy was applied to study LG NW FETs in different operation regimes in an $MgCl_2$ solution in the dark and under IR optical excitation. The high photosensitivity of the parameters of RTS fluctuations to infrared radiation was revealed. The parameters of RTS fluctuations can be effectively tuned by optical excitation. This represents a new approach for the optimization of characteristic times: capture and emission times and the dimensionless *R*-factor parameter to obtain enhanced bio-sensitivity in liquid-gated NW FET device structures. The method is based on the utilization of single-trap phenomena and is associated with these dynamic fluctuations measured in the form of RTS noise characteristics. New time characteristics and their dependence on the potential of the dielectric surface as well as on optical excitation can be analyzed to obtain significantly enhanced sensitivity of FET biosensors. The parameters can be fine-tuned without changing external voltages. It was demonstrated that high sensitivity of the parameters of RTS fluctuations to infrared radiation can be achieved. The sensitivity of FET biosensors can be amplified by 1.56 times under light excitation compared to the amplification coefficient obtained in the dark. The obtained results can also be applied to different areas of research and development of LG NW FET structures, including digital signal analyzing systems and biosensing applications.

4. Experimental Section

Liquid-gated Si NW FETs were fabricated using a complementary metal–oxide–semiconductor (CMOS)-compatible top-down approach. CMOS technology is widely used in industry production, therefore this technology is promising for the realization of new kinds of devices, including biosensors.[2,3,5,7,11] Additional arguments for using silicon nanowires are following a) robust manufacturability, the cheapest technology, and compatibility with microcircuits; b) small sizes; c) reaction rate; d) the possibility of using the stochastic characteristics of RTS fluctuations as sensitive parameters, which significantly increases the sensitivity of the sensor based on Si-NW and makes it possible to overcome the thermal limit of sensitivity. e) The size of a silicon nanowire could reach several tens of nanometers, therefore even a single biomolecule could significantly affect its electrical state.

The fabrication process starts by thinning down to 50 nm silicon-on-insulator (SOI) wafers purchased from SOITEC with a 70-nm-thick initially active Si layer. To pattern the nanowires, electron beam lithography was used. In the next step, a SiO_2 layer grown on top of the active Si layer was patterned using photolithography to obtain the mask for nanowire fabrication. Atomically flat nanowires were obtained using tetramethylammonium hydroxide (TMAH) wet chemical etching to transfer the NW pattern in SiO_2 to silicon. Ion implantation was then performed with boron ions to form ohmic feed line contacts to nanowires after the metal deposition. The nanowire channels were covered by an 8-nm-thick SiO_2 layer, which was thermally grown to serve as a gate dielectric. The source and drain contacts were highly implanted with boron ions, resulting in a p^+–p–p^+ structure. After metal deposition, the contact regions were protected with PI-2545 polyimide and cured to create a stable passivation and to prevent a shortcut between the contacts in a liquid. After the fabrication process, patterned wafers were cut into chips, wire bonded to chip carriers, and subsequently encapsulated with polydimethylsiloxane (PDMS) and glass rings to form a reservoir for biochemical liquids. Liquid-gate voltage was applied to the sample using a commercially available Ag/AgCl pellet reference electrode immersed in the $MgCl_2$ solution. The drain current fluctuations of NW FET devices were studied with and without external optical excitation in different regimes defined by drain-source biases and gate voltages to understand the single-trap characteristics. Noise spectra were obtained using the experimental setup developed in-house in the frequency range from 1 Hz to 100 kHz.

The light source was selected to excite the structures, with a photon energy of 1.3 eV exceeding the indirect bandgap of silicon, using the IR383 LED from EVERLIGHT (Taiwan). By considering the linear dependence of the radiation intensity on the current through the LED, the radiation intensity was regulated by the change in current and the distance between the light diode and an LG FET.

Statistical Analysis: Transport and noise properties of FET biosensors with 100 nm width and 200 nm length were investigated in 10^{-6} $MgCl_2$ solution. For electrical properties, the transfer and output characteristics of the FETs were studied using the *I–V* measurement system. Several noise spectra of nanowire biosensors are recorded using an ultra-low noise

measurement setup to analyze noise spectra. The original noise data were voltage spectral density, $S_v(f)$, measured as a function of frequency:

$$S_v(f) = \frac{1}{t_M}\left|F[v(t)](f)\right|^2 \tag{16}$$

where t_M is the duration time of the measurments, $F[v(t)](f)$ is the Fourier transform of time dependent of voltage signal, v(t).

The thermal noise was estimated as the voltage variance per hertz of bandwidth using the following equation:

$$S_{V\_Thermal}(f) = 4kTR_{eq} \tag{17}$$

where k was the Boltzmann constant, T was the temperature, and R_{eq} was the equivalent resistance.

The spectrum of thermal noise was subtracted from the measured one as follows:

$$S_{v,real}(f) = S_v(f) - 4kTR_{eq} \tag{18}$$

For further analysis, the spectral density of current fluctuation was corrected by the formula:

$$S_I(f) = \frac{S_{v,real}(f)}{R_{eq}^2}\left[\frac{1}{1+\left(\frac{f}{f_0}\right)^2}\right]^{-1} \tag{19}$$

where f_0 was the corner frequency which results from the presence of parasitic capacitance shunting the input of the preamplifier.

The noise spectra were analyzed after recording of at least 100 spectra. In this case, the accuracy could be estimated using the following equation:

$$\varepsilon = \frac{1}{\sqrt{\Delta f_{\min}\cdot t_M}} \tag{20}$$

where ϵ was the measurement error, $\Delta f_{\min}$ was the minimum width of the frequency bandwidth, Hz, t_M was the duration time of the measurement, s.

In this case, $\Delta f_{\min} = 1$ Hz, $t_M = \Delta t \cdot N = 100$ s, where $\Delta t = 1$ s was the duration of a single measurement, $N = 100$ was the number of accumulated spectra.

Using Equation (20) $\varepsilon = \frac{1}{\sqrt{1\cdot 100}} = 0.1$ thus was obtained, and the maximal value of accuracy was estimated to be ≈10%.

Acknowledgements

Silicon nanowire devices were fabricated at the Helmholtz Nano Facility (HNF) of Forschungszentrum Jülich. M.P. is grateful for a research grant from the Helmholtz Initiative and Networking Funds. M.P. would also like to thank Dr. W. Albrecht from the Helmholtz Nano Facility (HNF) of Forschungszentrum Jülich for supporting the research grant. Y.Z. and H.L. are very grateful for the research grant obtained from the China Scholarship Council (CSC).

Open access funding enabled and organized by Projekt DEAL.

Conflict of Interest

The authors declare no conflict of interest.

Data Availability Statement

The data that support the findings of this study are available from the corresponding author upon reasonable request.

Keywords

bioelectronics, liquid-gated field-effect transistors, nanowire, optical infrared excitation, two-level fluctuations

Received: August 4, 2023
Revised: November 23, 2023
Published online: January 9, 2024

[1] P. Bergveld, *IEEE Trans. Biomed. Eng.* **1972**, *19*, 342.
[2] F. Patolsky, G. Zheng, C. M. Lieber, *Nat. Protoc.* **2006**, *1*, 51.
[3] K.-I. Chen, B.-R. Li, Y.-T. Chen, *Nano Today* **2011**, *6*, 131.
[4] G. Shen, P.-C. Chen, K. Ryu, C. Zhou, *J. Mater. Chem.* **2009**, *19*, 828.
[5] C. M. Lieber, Z. L. Wang, *MRS Bull.* **2007**, *32*, 99.
[6] L. Ten Siethoff, M. Lard, J. Generosi, H. S. Andersson, H. Linke, A. Månsson, *Nano Lett.* **2014**, *14*, 737.
[7] R. Sivakumarasamy, R. Hartkamp, B. Siboulet, J.-F. Dufrêche, K. Nishiguchi, A. Fujiwara, N. Clément, *Nat. Mater.* **2018**, *17*, 464.
[8] S. Pud, A. Kisner, M. Heggen, D. Belaineh, R. Temirov, U. Simon, A. Offenhäusser, Y. Mourzina, S. Vitusevich, *Small* **2013**, *9*, 846.
[9] J. Li, Y. Kutovyi, I. Zadorozhnyi, N. Boichuk, S. Vitusevich, *Adv. Mater. Inetrf.* **2020**, *7*, 2000508.
[10] N. Clément, K. Nishiguchi, J. F. Dufreche, D. Guerin, A. Fujiwara, D. Vuillaume, *Appl. Phys. Lett.* **2011**, *98*, 014104.
[11] O. Knopfmacher, A. Tarasov, W. Fu, M. Wipf, B. Niesen, M. Calame, C. Schönenberger, *Nano Lett.* **2010**, *10*, 2268.
[12] Y. Kutovyi, J. Li, I. Zadorozhnyi, H. Hlukhova, N. Boichuk, D. Yehorov, M. Menger, S. Vitusevich, *MRS Adv.* **2020**, *5*, 835.
[13] A. Tarasov, M. Wipf, R. L. Stoop, K. Bedner, W. Fu, V. A. Guzenko, O. Knopfmacher, M. Calame, C. Schönenberger, *ACS Nano* **2012**, *6*, 9291.
[14] S. Pud, J. Li, V. Sibiliev, M. Petrychuk, V. Kovalenko, A. Offenhäusser, S. Vitusevich, *Nano Lett.* **2014**, *14*, 578.
[15] S. Pud, F. Gasparyan, M. Petrychuk, J. Li, A. Offenhäusser, S. A. Vitusevich, *J. Appl. Phys.* **2014**, *115*, 233705.
[16] J. Li, S. Pud, M. Petrychuk, A. Offenhäusser, S. Vitusevich, *Nano Lett.* **2014**, *14*, 3504.
[17] Y. Kutovyi, I. Zadorozhnyi, V. Handziuk, H. Hlukhova, N. Boichuk, M. Petrychuk, S. Vitusevich, *Nano Lett.* **2018**, *18*, 7305.
[18] Y. Kutovyi, I. Zadorozhnyi, H. Hlukhova, V. Handziuk, M. Petrychuk, A. Ivanchuk, S. Vitusevich, *Nanotechnology* **2018**, *29*, 175202.
[19] Y. Kutovyi, I. Zadorozhnyi, V. Handziuk, H. Hlukhova, N. Boichuk, M. Petrychuk, S. Vitusevich, *Phys. Status Solid.* **2019**, *256*, 1800636.
[20] Y. Kutovyi, V. Piatnytsia, N. Boichuk, I. Zadorozhnyi, J. Li, M. Petrychuk, S. Vitusevich, *Adv. Electron. Mater.* **2021**, *7*, 2000858.
[21] Y. Kutovyi, H. Hlukhova, N. Boichuk, M. Menger, A. Offenhäusser, S. Vitusevich, *Biosens. Bioelectron.* **2020**, *154*, 112053.
[22] Y. Kutovyi, I. Madrid, I. Zadorozhnyi, N. Boichuk, S. H. Kim, T. Fujii, L. Jalabert, A. Offenhaeusser, S. Vitusevich, N. Clément, *Sci. Rep.* **2020**, *10*, 12678.
[23] R. Yamanaka, Y. Shindo, K. Oka, *Int. J. Mol. Sci.* **2020**, *20*, 3439.
[24] Y. Hu, Z. Chen, Z. Hou, M. Li, B. Ma, X. Luo, X. Xue, *Molecules* **2020**, *24*, 2091.
[25] M. Petrychuk, S. Vitusevich, *Phys. Status Solid. Applicat. Mater. Sci.* **2022**, *220*, 2200619
[26] N. B. Lukyanchikova, B. Jones, *Noise Research in Semiconductor Physics*, CRC Press, Boca Raton, FL **2020**.
[27] N. R. Hall, *Phys. Rev. B* **1952**, *87*, 387.
[28] W. Shockley, W. T. Read, *Phys. Rev. B* **1952**, *87*, 835.

[29] Z. Çelik-Butler, in *Advanced Experimental Methods For Noise Research in Nanoscale Electronic Devices*, Springer, Dordrecht, **2004**, pp. 219–226.
[30] M. Schulz, *J. Appl. Phys.* **1993**, *74*, 2649.
[31] H. H. Mueller, D. Wörle, M. Schulz, *J. Appl. Phys.* **1994**, *75*, 2970.
[32] S. Birner, C. Uhl, M. Bayer, P. Vogl, *J. Phys.: Conf. Ser.* **2008**, *107*, 012002.